Measurement of the Branching Ratios $(K_L^0 \to \pi\mu\nu)/(K_L^0 \to \pi e\nu)$ and $(K_L^0 \to \pi^+\pi^-\pi^0)/(K_L^0 \to \text{all charged})$ Using a Heavy-Liquid Bubble Chamber*

G. R. Evans, J. Muir, and K. J. Peach
University of Edinburgh, Edinburgh, Scotland

and

I. A. Budagov,† H. W. K. Hopkins, W. Krenz,‡ F. A. Nezrick,§ and R. G. Worthington‖
CERN, Geneva, Switzerland

(Received 13 October 1971)

More than 4000 examples of K_L^0 charged decays have been observed in a heavy-liquid bubble chamber. The branching ratios have been measured to be $R_1 = (K_L^0 \to \pi\mu\nu)/(K_L^0 \to \pi e\nu) = 0.662 \pm 0.030$ and $R_2 = (K_L^0 \to \pi^+\pi^-\pi^0)/(K_L^0 \to \text{all charged modes}) = 0.159 \pm 0.010$.

I. INTRODUCTION

In recent years there has been considerable theoretical and experimental interest[1] in the semileptonic branching ratio $(K \to \pi\mu\nu)/(K \to \pi e\nu)$, for both K^+ and K_L^0 mesons. Much of this interest has centered around the observation that, using rather general assumptions, the branching ratios may be used to derive a value for ξ, the ratio of the form factors in the matrix element for the decay, which may also be determined from a study of Dalitz-plot distributions and polarization of the muon in $K_{\mu 3}$ decay. The increased statistical precision of experiments has led to a clearly defined difference between Dalitz-plot and branching-ratio determinations of ξ, on the one hand, and polarization determinations, on the other. The possibility that different results for ξ may be an indication of a breakdown in one of the basic assumptions regarding the nature of the decay interaction led to the undertaking of the measurement described in this paper.

The theoretical framework of the semileptonic K decay within the current-current theory with $V-A$ interaction has been extensively developed and summarized elsewhere.[2] In brief, for the decay $K_L^0(P) \to \pi(Q) + l(p) + \nu(q)$, the decay amplitude is written as the product of a hadronic current J and a leptonic current j,

$$M = (G \sin\theta/\sqrt{2}) J_\lambda j_\lambda , \tag{1.1}$$

where the lepton current has the general form $j = \bar{u}_l(p) O_i (1+\gamma_5) u_\nu(q)$, the O_i representing some combination of the S, V, T, A, and P bilinear forms. Since the kaon and pion are both pseudoscalar mesons, only S, V, and T transitions are allowed, and the possible forms for the K-π transition matrix element are

$$f_S P_\lambda Q_\lambda , \quad f_+(P+Q)_\lambda + f_-(P-Q)_\lambda , \quad f_T P_\lambda Q_\sigma ,$$

where the f_i are the form factors, in general complex. If the leptons are locally produced the form factors are functions only of t, the squared four-momentum transfer to the dilepton system. [$t = (P-Q)^2 = (p+q)^2$, the invariant mass squared of the lepton pair.]

Lorentz invariance of the decay amplitude then restricts the form of the operators O_i to be S, V, and T, respectively. If the decay interaction is assumed to be purely $V-A$ (i.e., $f_S = f_T = 0$), Eq. (1.1) may be written as

$$M = (G \sin\theta/\sqrt{2})[f_+(t)(P+Q)_\lambda + f_-(t)(P-Q)_\lambda]\bar{u}_l(p)\gamma_\lambda(1+\gamma_5)u_\nu(q) .$$

Writing $f_-(t)/f_+(t)$ as $\xi(t)$, time-reversal invariance requires that $\xi(t)$ is real. (The effects of time reversal noninvariance are known to be small in K_{e3} decays.) The form factors $f_\pm(t)$ are usually expanded in a power series about $t=0$, i.e.,

$$f_\pm(t) = f_\pm(0)[1 + \lambda_\pm t/m_\pi{}^2 + \cdots] ,$$

and if λ_+ is small, we may write

$$\xi(t) = \xi(0)[1 + (\lambda_- - \lambda_+) t/m_\pi{}^2 + \cdots] .$$

With the foregoing assumptions, evaluation of the decay matrix element leads to a decay differential distribution of the form

$$\rho(E_\pi, E_l)dE_\pi dE_l = (G^2 \sin^2\theta/16\pi^3)|f_+(t)|^2[m_K(2E_lE_\nu - m_K E_\pi') + \tfrac{1}{4}m_l{}^2E_\pi' - m_l{}^2E_\nu + m_l{}^2(E_\nu - \tfrac{1}{2}E_\pi')\xi(t) + \tfrac{1}{4}m_l{}^2E_\pi'\xi(t)^2]dE_\pi dE_l\,, \quad (1.2)$$

where $E_\pi' = E_{\pi,\max} - E_\pi$.

It is clear that in K_{e3} decay, terms containing $m_e{}^2$ are negligible, removing the dependence of $\rho(E_\pi, E_e)$ on ξ, while in $K_{\mu3}$ all terms remain. Thus measurements of the Dalitz plot yield a value for $f_+^e(t)$ in K_{e3} decay, and values for $f_+^\mu(t)$ and $f_-^\mu(t)$ in $K_{\mu3}$ decay. Further, if muon-electron universality is assumed, then $f_\pm^e = f_\pm^\mu$, and integration of the differential distributions allows the branching ratio R_1 to be related to the parameters $\xi(0)$, λ_+, and λ_-. The explicit relationship is deferred to Sec. V.

In the phenomenological description of $K_{3\pi}$ decays there are only two independent variables, which may be chosen to be $(T_+ - T_-)$ and T_0 (the subscript refers to the charge of the pion). In the limit of exact CP invariance there can be no dependence on odd powers of $(T_+ - T_-)$, so that the matrix element may be written as

$$M \sim 1 + \sum_{j=1}^{\infty}\left[a_j \frac{m_K}{m_{\pi^+}{}^2} T_{\max}\left(\frac{2T_0}{T_{\max}} - 1\right)^j + b_{2j}\frac{m_K}{m_{\pi^+}{}^2}(T_+ - T_-)^{2j}\right], \quad (1.3)$$

with $T_{\max}$ the maximum energy of the π^0 in the K_L^0 rest system. Because of the smallness of the physical region, the series may be truncated after only a few terms. Assuming that the *squared* matrix element is linear in T_0, the expression for the reduced π^0 energy spectrum (the energy spectrum divided by phase space) becomes

$$\phi(T_0)dT_0 \sim \left[1 + 2a_0\frac{m_K}{m_{\pi^+}{}^2}T_{\max}\left(\frac{2T_0}{T_{\max}} - 1\right)\right]dT_0\,. \quad (1.4)$$

In the literature there are many variants of Eqs. (1.3) and (1.4), depending upon assumptions regarding both the linearity of the spectrum or matrix element and the position of the "center" of the Dalitz plot (which is not well defined in these decays).

We present here a full account of a direct measurement of the branching ratios $(K_L^0 \to \pi\mu\nu)/(K_L^0 \to \pi e\nu)$ and $(K_L^0 \to \pi^+\pi^-\pi^0)/(K_L^0 \to \text{all charged})$, in which there was an almost complete separation of the decay modes, and in which the ξ and a_0 dependence of the corrections was significantly smaller than the purely statistical error. The result has been reported elsewhere.[3] In Sec. II we briefly discuss the exposure, and present in some detail the scanning rules and track identification procedures employed. Section III deals with the definition of the fiducial region for the case in which the decay vertex is not seen, and where there is no attempt to reconstruct the event. In Sec. IV the corrections to the data are discussed, and Sec. V compares these results with those of other experiments.

II. EXPERIMENTAL PROCEDURES

A. The Exposure

Full details of the exposure and beam have been given elsewhere.[4] In brief, a neutral beam was taken at 30° from an internal beryllium target at the CERN Proton Synchrotron. Approximately 7×10^{10} protons per pulse impinged on the target, at an incident momentum of 19.2 GeV/c. The beam line is shown diagrammatically in Fig. 1. The distance from the target to the center of the chamber was 22.5 m, and for the last 13 m the beam was transported *in vacuo* (4×10^{-2} Torr pressure of air).

The beam was restricted to a solid angle of 4.5×10^{-7} sr by three 3-m-long collimators. At the chamber the beam had a 2-cm-diameter profile[5] [shown in Fig. 2(a)], and was composed on the average of 50 K_L^0, 7×10^2 γ rays (with energy >1 GeV), and 3.5×10^3 neutrons (with kinetic energy >0.3 GeV) per pulse.[6] The momentum spectrum of the decaying K_L^0, determined[5] from the measurements of $K_L^0 \to \pi^+\pi^-\pi^0$ ($K_{3\pi}$) decays, is shown in Fig. 2(b).

The chamber used was the CERN heavy-liquid bubble chamber, 1.2 m in diameter and 1.0 m deep, filled with heavy Freon, CF_3Br (radiation length 11 cm and natural collision length 58 cm), and having a magnetic field of 27 kG. A vacuum pipe to contain the K_L^0 beam was fitted across the chamber diameter some 60 cm from the liquid side of the front glass. About 800 000 photographs were obtained with an average of 1.5 K_L^0 decays/photograph.

The chamber vacuum pipe was of 0.25-cm-thick aluminum, and had an internal diameter of 4 cm. At the end where the beam entered, the pipe was fitted with a lead collar 20 cm in diameter and 10 cm thick, to reduce the number of charged particles and γ rays entering the liquid from decays occurring just before the chamber. Two marks were painted around the pipe, one 5 cm from the face of the lead collar and the other 55 cm from it. A mirror suspended freely from the back plate of the chamber close to the diaphragm and some 35

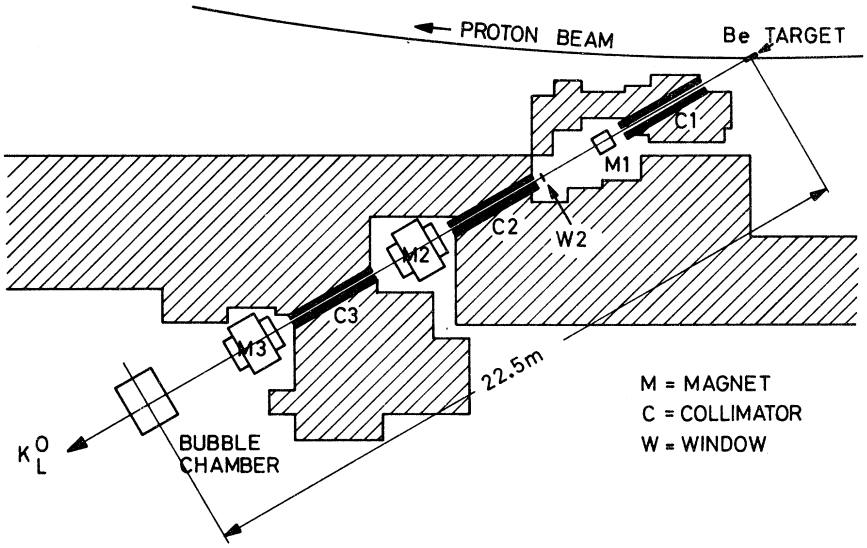

FIG. 1. Plan of beam line.

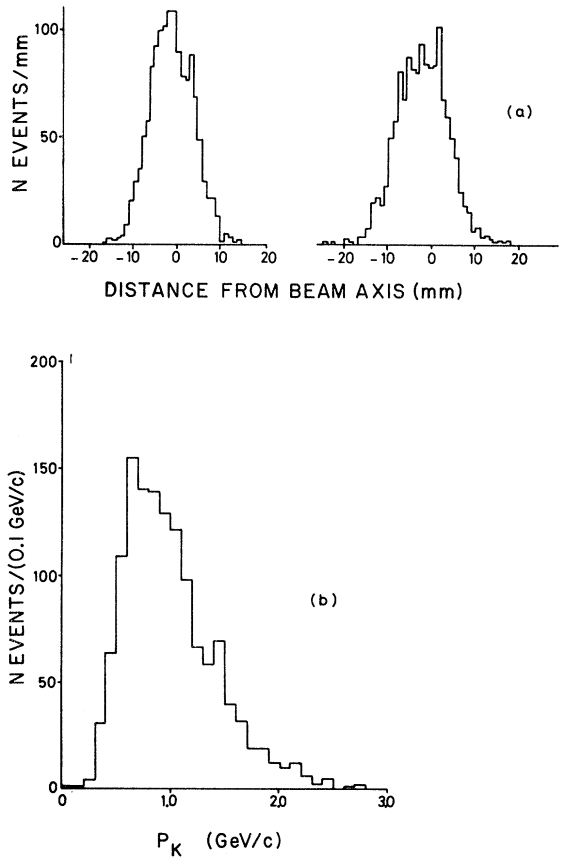

FIG. 2. (a) Profile of the K_L^0 beam at the chamber, obtained from measurements of $K_{3\pi}$ decays. (b) Apparent momentum spectrum of the decaying K_L^0, obtained from measurements of $K_{3\pi}$ decays.

cm behind the pipe made it possible to observe tracks which would otherwise have been hidden. A diagrammatic representation of the configuration in the chamber is shown in Fig. 3.

B. Scanning Criteria and Track Identification

The K_L^0 has four principal decay modes, namely

$$\left.\begin{aligned} K_L^0 &\to \pi\mu\nu\text{:} \quad K_{\mu 3} \\ K_L^0 &\to \pi e\nu\text{:} \quad K_{e3} \end{aligned}\right\} K_{l3}$$

$$K_L^0 \to \pi^+\pi^-\pi^0\text{:} \quad K_{3\pi}$$

$$K_L^0 \to \pi^0\pi^0\pi^0\text{:} \quad K_{3\pi^0}\,.$$

In this experiment, interest was centered on the charged decay modes, and no attention was paid to $K_{3\pi^0}$ decays, which were excluded by the scan rules. The detection of the charged modes $K_{\mu 3}$, K_{e3}, and $K_{3\pi}$ required the observation of "heavy" tracks, such as are normally made by pions or muons, "electronic" tracks, such as are normally made by electrons, and "γ rays," as evidenced by conversion pairs or Compton electrons.[7] Since the charged particles were only observed after leaving the pipe, it was necessary to associate their observed tracks and γ rays, if any, with a single decay of the K_L^0. This association of tracks became difficult and unreliable when there were several decays on the same photograph, and although it would have been possible to formulate scan rules so that the constituents of different decays were separated by some minimum distance, it would have been difficult to do this in a way

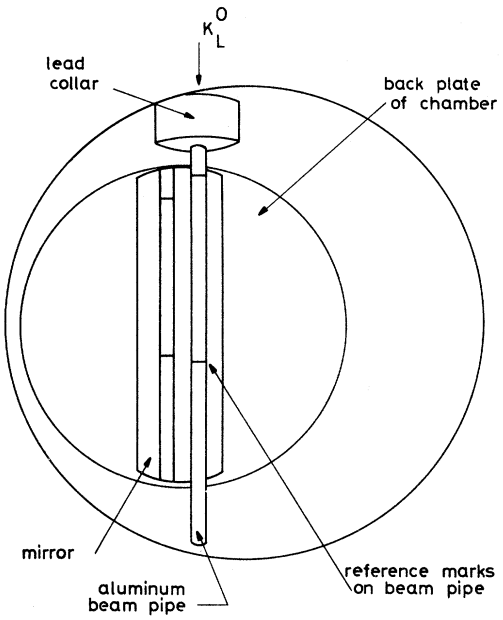

FIG. 3. Schematic diagram of the bubble chamber.

which would have yielded an unbiased sample of decays, while keeping the scan rules simple enough to allow efficient scanning. Moreover, it was difficult to scan those frames containing more than one decay, in which electrons or γ rays giving bremsstrahlung showers intermingled or obscured features of the other decays. On the other hand, rapid and unbiased scanning should be expected if attention was limited to frames containing just one decay, and charged decay candidates were therefore selected according to this latter criterion.

The scan rules were formulated not simply to collect those frames containing perfect examples of the recognized decay modes, but rather to reject only those frames on which there was definite evidence for more than one decay. In this way all possible examples of single decays could be obtained, no matter how degenerate, as well as sufficient additional information to allow corrections to be estimated. Thus, a frame was rejected only if it showed three or more tracks leaving the pipe or evidence of more than three γ rays originating within the pipe, at any point along its length between the face of the lead collar at $x=-5$ cm and $x=+86$ cm.[8] Tracks or γ rays emerging from the face of the lead collar caused a frame to be rejected, but those which left the pipe beyond $x=+86$ cm, or which left the side of the lead collar, or were electrons which could be contained within a 3-cm-diameter circle, did not do so.

The remaining frames contained a single "event." In this context an "event" was defined as one track, or two tracks of particles of the same or opposite sign, together with up to three conversion pairs or Compton electrons, not counting those which had arisen from bremsstrahlung or pion interaction. To be accepted, the charged tracks were required to leave the pipe in a fiducial region extending from $x=0$ to $x=+68$ cm. By using a longer length of the pipe when considering a frame for validity and a shorter one when collecting the tracks of an event, a guard region was introduced at either end of the fiducial length used in scanning. There was no demand that the charged particles forming an "event" come from a recognized decay mode of the K_L^0, nor even from a single vertex. Nevertheless, a frame was rejected when the spatial arrangement of converted γ rays indicated an origin within the pipe inconsistent with any reasonable location of the origin of the charged tracks.

It was recognized that the rejection of frames because of the criterion of nonassociated γ rays might lead to a bias against difficult events, since it was more likely that small γ rays would be observed in the more intensive study required by a difficult picture. In addition, electron pairs become increasingly difficult to "point" correctly as their energy decreases, so the association of such γ rays with the possible origin of the charged tracks was unreliable. For these reasons, the presence of unassociated electron pairs or Compton electrons caused a rejection only when their energy was greater than about 20 MeV. This energy boundary was defined in terms of a circle of 3.0-cm diameter; to be effective in the rejection of a frame, electron pair or Compton electron tracks had to be more extensive than could be contained within this standard circle. Otherwise, they were ignored.

Conversion pairs in the pipe wall were accepted if the separation of the points of exit of the branches from the pipe was less than 1 cm. However, a frame was rejected when a pion interacted in the pipe wall before entering the liquid and gave more than one visible charged secondary track.

Some 75 000 frames were double-scanned, and about 10% satisfied the criteria for validity. For each valid photograph, the scanner recorded the point of exit from the pipe of each charged track, the characteristics of the track, and its length. The number of γ rays associated with the events were also recorded. All frames of questionable validity were retained by the scanner, and these frames, as well as those in which the charged tracks appeared incapable of coming from a common vertex, were flagged to draw the attention of the physicist.

The information for all recorded events from all

scans was entered on punched cards to allow automatic tabulation and comparison of data recorded for the same frame on different scans. The results of this process were passed to a physicist who, by inspection of the film, checked the validity of each frame recorded, whether by one or more scans, and then classified the tracks in each event according to a scheme based upon the characteristics of the tracks. It should be emphasized that the physicist looked at all frames recorded, even when there was a total agreement between the two scans. Each track was first examined for electronic characteristics, these being listed in (i) below. The remaining tracks were classified as "heavy" (the shorthand t is used for a heavy track in the remainder of this paper) and examined for the pion characteristics listed in (iia) below; those without such characteristics were not distinguishable between the pions and muons and were characterized by the features listed in (iib). Some tracks were difficult to classify definitely as "electronic" or "heavy" and at this stage were called "ambiguous". Often, ambiguous tracks were difficult to classify because a short range was allied with a large dip.

(i) The primary reason for classifying a track as electronic was the observation of conversion pairs or Compton electrons arising from bremsstrahlung from the track.[9] Total radiation or positron annihilation, in which the track was seen to end abruptly in the liquid with one or two γ rays pointing to its end and close to the forward direction, was taken as an electronic identifier. (The possibility that such signatures could have come from charged-pion interactions producing a neutral pion was investigated by studying the angular distribution of γ rays from such interactions. It was found that less than one pion in the entire sample would have been wrongly identified as electronic in this way.) In the absence of any converted bremsstrahlung the electronic nature of a track was inferred from rapid change in curvature of a lightly ionizing track,[9] or the observation of δ rays of such an energy as could only have been produced by an electron. A few tracks were classified as electronic because the observed range of the particle was completely inconsistent with the momentum calculated from the track curvature when the particle was assumed to be either a pion or a muon.

(iia) A track was classified as pionic when it was seen to lead to an interaction resulting in charged secondaries or possible conversion pairs indicative of neutral pion production. A high-momentum track which ended in the liquid without showing any increase in curvature or in ionization towards its end was taken to be the track of a pion which had interacted in flight producing no observed secondaries. The occurrence of a single scatter with a momentum transfer of more than 100 MeV/c was taken as evidence that the particle was a pion.[10] The observation of a possible π-μ-e chain was used as an identifier at this stage, but, in the final analysis, tracks identified this way were simply classed as "heavy" tracks because a study showed that this was not a reliable pion identification, since the length of the intermediate muon track in CF_3Br is only 1.4 mm.

(iib) The majority of "heavy" tracks, though clearly nonelectronic, could not be classified as pions rather than muons. The tracks in this class were those which left the chamber showing no scatter with momentum transfer greater than 100 MeV/c and those which, with heavy ionization at the end, stopped in the chamber without a decay being seen,[11] or decayed into an electron track with no evidence of an intermediate muon.

A detailed discussion of the consistency of track identification and classification is given in Sec. IV A.

Having classified the tracks, the physicist prepared a final scan record, checking the information recorded by the scanners against the photograph and making alterations, deletions, and additions as they were required. When there were doubts about any aspect of the record, the physicist gave it a flag to indicate that it needed inspection by other physicists. A new set of punched cards was prepared from this record, and the information then available about each event was used to arrange them into the groups listed in Table I. Those events [12] that were not obviously from one of the principal decay modes, which were not single-track events, and those which had been flagged by the physicist as needing further attention, were reexamined. In this process some 6% of all events were restudied on the scan table by two or more physicists working together, and the record was amended where appropriate. After this final process, 7500 events of all categories were available for the analysis.

III. FIDUCIAL REGION

One of the major problems in obtaining a reliable and unbiased data set was the precise definition of the fiducial region, since the decay vertex was hidden within the pipe and could not be located with any great precision. While vertices could be found from measurements of those charged tracks and converted γ rays which formed the event, due to multiple scattering the individual track errors were quite large, and, given only a single geometrical constraint on the vertex, the reconstruction was not always reliable. For example, for $K_{3\pi}$ events, using only the tracks of the two

TABLE I. Event classification.

Class		Class characteristics	No. in class
1	K^0_{e3}	One electronic track, one nonelectronic track of opposite sign which may or may not be identified as a pion. No γ rays other than those consistent with bremsstrahlung.	1890
2	$K^0_{\mu 3}$	Two nonelectronic tracks, not more than one of which is identified as a pion. No γ rays.	1309
3	$K^0_{3\pi}$	Two nonelectronic tracks and one or two γ rays associated with the likely decay point.	558
4	$\pi^+\pi^-$	Two identified pion tracks and no γ rays.	8
5	e^+e^-	Two identified electronic tracks.	41
6	Single tracks	One track of any nature with or without associated γ rays (see also Table IV).	167
7	$K^0_{e3}+\gamma$	Same as K^0_{e3}, but with one associated γ ray not consistent with bremsstrahlung.	19
8	Unclassified	8.1 Two tracks, one nonelectronic and one ambiguous between electron scatter and muon or pion decay.	13
		8.2 One nonelectronic track, one track unidentified due to reentry into the pipe after very short length.	2
		8.3 One electronic track, one unidentified track as above.	1
		8.4 One nonelectronic track, one unidentified track as above, one associated γ ray.	1
9	Other categories	9.1 Two tracks of any nature with the same charge.	4
		9.2 Two tracks of any nature of opposite charge but recorded as unassociated.	4
		9.3 Same as K^0_{e3}, but with two associated γ rays not consistent with bremsstrahlung.	6
		9.4 Same as K^0_{e3}, but with three associated γ rays not consistent with bremsstrahlung.	2
		9.5 Same as $K^0_{3\pi}$, but with three associated γ rays.	1
		9.6 One or two electronic tracks and up to three γ rays.	11
	Total		4033

charged pions, the typical error on the decay vertex was ±2 cm in the beam direction[5]; reconstruction was considerably worse for K_{e3} events, and impossible for single-track events. The fiducial region was therefore defined in terms of a direct observable, requiring no reconstruction of the decay vertex.

For a pure K^0_L beam in a constant magnetic field with a pipe of negligible wall thickness, the distribution along the pipe of the exit point of, say, the upstream track (i.e., the first track to exit the pipe) of decays of the same configuration will be the same as the longitudinal distribution of the vertex points of these decays except for a displacement Δx in absolute position along the beam direction.[13] This holds true for decays of different configurations except that the displacements Δx_i will depend upon the configuration i. Thus to demand for all events that the exit point of the upstream track lie in a fixed region of the pipe of length l is to select the vertices of all events of all configurations to come from the same lengths l, although these lengths l have different displacements Δx_i in absolute position along the beam direction. For the small-diameter pipe and relatively high-momentum K^0_L used in this experiment, the actual displacements Δx_i are quite small [Figs. 4(a)–4(f), obtained from the Monte Carlo simulation, illustrate the correlation between exit point of the upstream track and vertex point for the different decay modes]. The difference between the Δx_i for different configurations is also very small. Because the differences between the $\langle \Delta x_i \rangle$ are small, the effect of attenuation of the beam by decay reducing the relative contribution of those events whose configuration leads to a small value of Δx_i

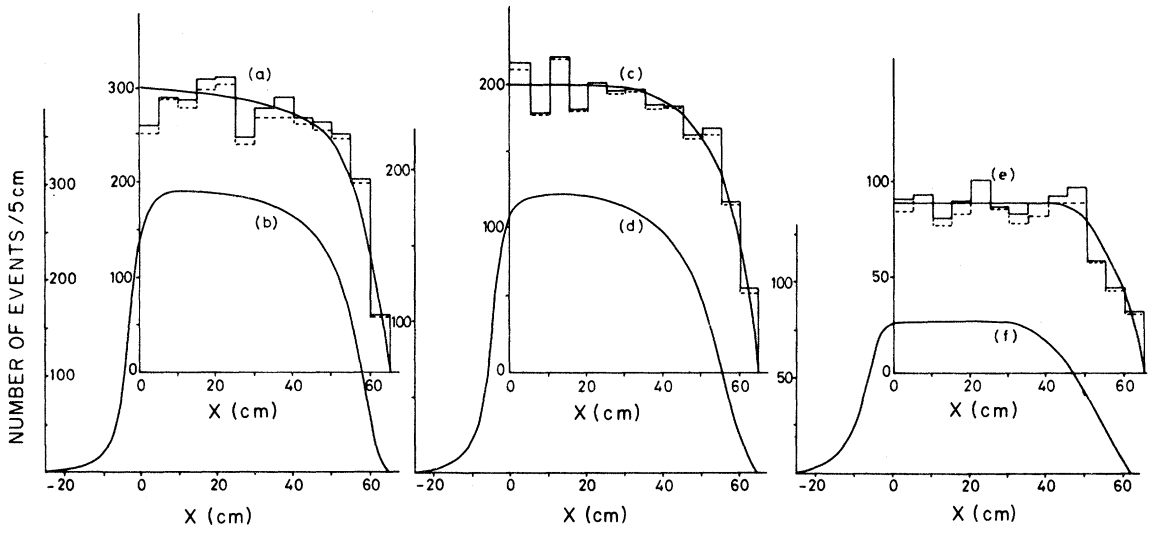

FIG. 4. (a), (c), (e) Distributions of the point of exit from the pipe of the upstream track for each of the three decay modes K_{e3}, $K_{\mu 3}$, and $K_{3\pi}$, respectively. The smooth curves represent the Monte Carlo predictions for these distributions, the broken histograms represent the original data, and the solid histograms represent the same distributions, corrected for scan efficiency. (b), (d), (f) Vertex-point distributions from the Monte Carlo simulation for those events in Figs. 4(a), 4(c), and 4(e).

is quite negligible. There will also be effects leading to a differentiation between the configurations due to the finite thickness of the pipe wall, but these are also small and calculable. It should be noted that in the limit of infinite extension of the apparatus this method is independent of the form of the decay matrix element, but, by requiring *both* tracks of an event to emerge from the pipe within a given region, small ξ-dependent and mode-dependent effects are introduced.

Thus, the events finally selected for analysis were those in which the upstream track of a two-track event or the lone track of a single-track event emerged from the pipe between 15 cm and 50 cm from the upstream mark, and in which the second track of a two-track event emerged less than 65 cm from this mark. The upstream limit was chosen to ensure that the vertices of selected events lay predominantly (>96% for $K_{3\pi}$ decays) within the chamber and downstream of the lead collar, minimizing possible misidentification of $K_{3\pi}$ decays as $K_{\mu 3}$ due to absorption of the γ in the lead, and giving close to full 4π geometry for all events. The downstream limits ensured that the potential length for all charged tracks was not less than 3 radiation lengths, and gave a geometrical detection efficiency of greater than 96% for K_{e3} and $K_{\mu 3}$, and greater than 99% for $K_{3\pi}$.

IV. CORRECTIONS TO THE DATA AND RESULTS

The number of events in each group satisfying the scan rules and the fiducial-volume limitations of Sec. III are given in Table I. These numbers required several small corrections before they could be used to evaluate the branching ratios. The corrections, which are discussed in detail below, were calculated using a combination of experimental data and information from a Monte Carlo simulation of the experiment; in the Monte Carlo calculations the parameters ξ and a_0 in the expression for the matrix elements in K_{l3} and $K_{3\pi}$ decays (see Appendix) were set as $\xi = 0.0$ and $a_0 = -0.24$. The corrections proved to be insensitive to the precise values chosen for ξ and a_0.

A. Scanning and Identification Efficiencies

The accuracy of this experiment was strongly dependent upon the scanning, and consequently some care was taken with the evaluation of the scanning efficiencies. The assumptions usually made about scanning efficiencies and about the nature of missed events were not necessarily valid in this case; the reader is referred to the paper by Derenzo and Hildebrand[14] for a general discussion of this point. As a necessary part of the evaluation of scanning efficiency, 15% of the total film scanned by each participating laboratory was transferred to the other, where it was completely and independently reprocessed. Afterwards, a minute comparison was made between the records kept by the two laboratories for this common film. All discrepancies were examined by a group of physicists containing representatives from each establishment, and the final assignment of every

event determined. Then, for each of the three decay modes $m_{1,2,3} = K_{e3}$, $K_{\mu 3}$, and $K_{3\pi}$, the events were divided into four categories:

(i) those events found and classified similarly by both laboratories (N_B^m),

(ii) those valid events found by only one of the two laboratories (N_L^m, L = laboratory 1 or 2),

(iii) those events recorded by one of the laboratories but which should not have been retained [usually for formal reasons connected with the rigorous application of the scan rules] (K_L^m), and

(iv) those events found by both laboratories but classified as belonging to different decay modes ($C_L^{m_i \to m_j}$).

TABLE II. Scanning and identification comparisons.

(a) Interlaboratory scan results
(L_1 = CERN, L_2 = Edinburgh)

	N_B^m	$N_{L_1}^m$	$N_{L_2}^m$	$K_{L_1}^m$	$K_{L_2}^m$
K_{e3} ($m=1$)	239	4	13	1	11
$K_{\mu 3}$ ($m=2$)	150	0	1	2	5
$K_{3\pi}$ ($m=3$)	64	5	10	4	2
Other ($m=4$) [a]	31	6	6	0	1

(b) Interlaboratory physicists' comparison

m_i \ m_j	$C_1^{m_i \to m_j}$ 1	2	3	4	m_i \ m_j	$C_2^{m_i \to m_j}$ 1	2	3	4
1	···	1	0	0	1	···	1	0	4
2	0	···	1	0	2	2	···	1	1
3	0	0	···	0	3	1	2	···	0
4	1	0	0	···	4	3	1	0	···

(c) Three-scan results [b]

Mode	M_1	M_2	M_3	ϵ_1	ϵ_1'	ϵ_2	ϵ_2'
K_{e3}	386	33	10	0.925	0.876	0.995	0.951
$K_{\mu 3}$	280.7	14.3	4	0.950	0.925	0.998	0.973
$K_{3\pi}$	110	13	5	0.890	0.792	0.988	0.885
Other	60.3	12.3	7.3	0.825	···	0.969	···

[a] $m=4$ represents all those events not directly classifiable as K_{e3}, $K_{\mu 3}$, $K_{3\pi}$.

[b] The notation in (c) is as follows: M_1 = mean number of events found by a single scan. M_2 = mean number of events missed by one scan out of three. M_3 = mean number of events missed by two scans out of three. ϵ_n = efficiency of n scans assuming that events are missed randomly. ϵ_n' = efficiency of n scans using the method of Ref. 14, taking into account possible biased loss of events. The expression employed was $\epsilon_n' = N_n/N_T$, where N_n = number of events found by n scans and $N_T = M_1(\alpha+\beta+2)/(\alpha+1)$. α and β were evaluated from $\beta = (K_{12} - 2K_{23} + 1)/(K_{23} - K_{12})$, $\alpha = K_{12} - 3 + (K_{12} - 1)\beta$, where $K_{12} = M_1/M_2$, $K_{23} = M_2/M_3$. These expressions are only valid for $\alpha, \beta > -1$, which is not satisfied by the data in the fourth line of the table.

The results are shown in Table II. It can be seen immediately that there was some difference in the scanning efficiencies between the principal modes, these being several percent lower for K_{e3} and $K_{\pi 3}$ than for $K_{\mu 3}$. This was probably due to the general increase in the complexity of the appearance of events when electrons and γ rays gave large showers, in marked contrast to the relatively clean appearance of the majority of $K_{\mu 3}$ events.

The scanning efficiency for each laboratory and for each mode was calculated from the expression

$$\epsilon_{L_1}^m = \frac{N_B^m}{N_B^m + N_{L_2}^m}; \quad \Delta\epsilon_{L_1}^m = \left(\frac{\epsilon_{L_1}^m (1 - \epsilon_{L_1}^m)}{N_B^m + N_{L_2}^m}\right)^{1/2},$$

where it was assumed that the scans made by the two laboratories on the interchanged film were independent, and that the events remaining unseen after two scans in each laboratory were missed randomly. This was not rigorously true, but the errors introduced were negligible because the individual double-scanning efficiencies were high. The results of these calculations are given in Table III.

As an independent check on the above method, a 30% third scan was performed, and all new events were classified by a physicist as before. The scan efficiencies were then computed using the method of Derenzo and Hildebrand,[14] with the results given in Table II(c) and the third column of Table III. It may be seen that the two methods gave efficiencies in good agreement for all modes.

The exchange of film also made it possible to evaluate the extent to which tracks were misidentified by physicists. An effective physicist reliability was defined by

$$\epsilon_{P_L}^{m_i} = \frac{-K_L^{m_i} - \sum_{m_j} (C_L^{m_i \to m_j} - C_L^{m_j \to m_i})}{N_B^{m_i} + N_L^{m_i} + K_L^{m_i} + \sum_{m_j} C_L^{m_i \to m_j}}$$

and evaluated for each laboratory. The averages over the various physicists concerned are given in Table III. The values obtained represented the subtraction to be applied to each mode resulting from the tendency of the physicist to accept invalid events $K_L^{m_i}$, and to misidentify valid events $C_L^{m_i \to m_j}$.

The scan and identification efficiencies for the individual laboratories were combined to give an over-all efficiency for each decay mode using

$$\epsilon_{T_L}^m = \epsilon_L^m / (1 + \epsilon_{P_L}^m).$$

These results are given in the last column of Table III. The data for each laboratory were corrected for this over-all efficiency before the two data sets were combined. All other corrections were applied to the combined set of data.

TABLE III. Summary of scanning and identification efficiencies.

	Scanning comparison (double-scan efficiency) $\epsilon^m_{L_1}$	$\epsilon^m_{L_2}$	Double-scan efficiency derived from third scan	Physicists' identification reliability $\epsilon^m_{pL_1}$	$\epsilon^m_{pL_2}$	Combined scan and efficiency identification reliability $\epsilon^m_{\pi L_1}$	$\epsilon^m_{\pi L_2}$	Over-all efficiency for total data normalized to 100% for $K_{\mu 3}$ decays
K_{e3}	0.948 ± 0.014	0.984 ± 0.014	0.951 ± 0.005	−0.004 ± 0.014	−0.037 ± 0.044	0.952 ± 0.020	1.021 ± 0.020	0.964 ± 0.021
$K_{\mu 3}$	0.993 ± 0.008	1.000 ± 0.008	0.973 ± 0.004	−0.013 ± 0.010	−0.031 ± 0.010	1.008 ± 0.013	1.031 ± 0.013	1.000
$K_{3\pi}$	0.865 ± 0.035	0.928 ± 0.035	0.885 ± 0.028	−0.041 ± 0.025	−0.050 ± 0.025	0.901 ± 0.040	0.978 ± 0.040	0.919 ± 0.037

B. Geometrical Detection Efficiency

As mentioned in Sec. III, the downstream cut on the exit point from the pipe of the downstream track required a mode-dependent correction to the data. This effect was studied using the Monte Carlo simulation. To show that this simulation was adequate to describe the data, the exit point distributions of the upstream track were compared with those predicted by the Monte Carlo simulation in Figs. 4(a)–4(f). [The exit-point distribution of the data was corrected for scanning efficiency by the addition of events found in the third scan appropriately weighted into the various intervals. This is in the upper (solid line) histogram in Figs. 4(a), 4(c), and 4(e).] The χ^2 fits of the Monte Carlo-generated distributions to the data were, for 12 degrees of freedom in each case, 21.8 for K_{e3}, 9.8 for $K_{\mu 3}$, and 10.5 for $K_{3\pi}$.

The loss of events at the downstream end arose partly through the rejection of frames where the downstream track left the pipe in the "guard region" from 65 to 86 cm, and partly through events being classed as single-track events where the second track emerged downstream from the 86-cm limit. To calculate the required correction, 50 000 events of each mode were generated with their vertices uniformly distributed in the region from −35 cm to +70 cm relative to the upstream mark. In the fiducial region used in this analysis 13 213 K_{e3}, 13 184 $K_{\mu 3}$, and 13 698 $K_{3\pi}$ events were accepted. The difference between $K_{\mu 3}$ and K_{e3} is statistically insignificant (in a rerun, using a different set of random numbers, 13 297 $K_{\mu 3}$ were accepted) and no correction was made to these modes, but (3.5 ± 1.0)% was subtracted from the $K_{3\pi}$ mode.

C. γ-Detection Efficiency, *CP*-Violating $\pi^+\pi^-$ Decay, Dalitz Pairs, and Compton Electrons on the Pipe

1. *γ-Detection Efficiency and $K_L^0 \to \pi^+\pi^-$ Decay*

Those $K_{3\pi}$ events in which neither γ ray from the π^0 was detected would have been classified as $K_{\mu 3}$ unless both the π^+ and the π^- were fully identified. The γ-ray detection efficiency was calculated from $\epsilon_\gamma = 2N_2/(2N_2 + N_1)$, where N_2 is the number of $K_{3\pi}$ events with both γ's detected and N_1 is the number of $K_{3\pi}$ events with only one γ detected. In making this calculation, it was assumed that the probability of detection of one γ ray from a π^0 was not dependent on the detection of the other. However, the probabilities of conversion of the two γ rays were not necessarily independent, because of the geometrical limitations of the chamber and pipe. The Monte Carlo study showed that the error introduced by neglecting this correlation was

less than 10% in the evaluation of this correction. Moreover, since the observation of one γ ray motivated the scanner to search more carefully for a second, some small correlation could have been introduced in the scanning, with opposite sense to the geometrical correlation. Neither of these effects was therefore included.

The experimentally observed values $N_1 = 112$ and $N_2 = 446$ gave $\epsilon_\gamma = 0.89 \pm 0.02$. Thus, 8 ± 2 genuine $K_{3\pi}$ events with no detected γ's would be expected. In addition, the data should contain 8 $\pi^+\pi^-$ events from the CP-violating decay of the K_L^0.[15] Hence this expected number of $\pi\pi$ events, viz., 16 ± 2, was subtracted from the sum of the total events classified as $K_{\mu 3}$ and $\pi^+\pi^-$.

2. *Dalitz Pairs*

Some genuine decays of the K_L^0 would have appeared in such a form that the frame would have been rejected at the scanning stage, because the scan rules rejected any frame with three or more charged tracks leaving the pipe. Thus, any $K_{3\pi}$ event which gave a Dalitz pair at the decay vertex would have been lost to the data. Using the value $(1.17 \pm 0.04)\%$ for the branching ratio $(\pi^0 \to e^+e^-\gamma)/(\pi^0 \to 2\gamma)$,[16] a loss of seven events from the $K_{3\pi}$ mode due to Dalitz pair production was calculated.

3. *Compton Electrons in the Pipe Wall*

Any event in which one of the γ rays gave rise to a single electron in the pipe wall was lost to the data through the proper application of the scan rules. To evaluate this effect, a special scan was performed for three charged-track events which had two nonelectron tracks, one electron track, and one or two γ rays. The γ rays were required to be associable with a possible origin of the nonelectron tracks, but there was no demand that the electron should appear to be associated. 44% of the film was scanned once; 26 such two-γ events and 20 such one-γ events were found. Assuming that all 26 two-γ events were genuine $K_{3\pi}$ events with an unassociated electron, and knowing the γ-detection efficiency, it was calculated that 7 ± 1 genuine one-γ $K_{3\pi}$ events with an extra electron should have been detected. The remaining 13 ± 5 events of the class were taken to be genuine two-γ $K_{3\pi}$ events, where one of the γ rays has converted in the pipe wall to give a single electron. This number was corrected for the scanning efficiency of a single scan for $K_{3\pi}$ events to yield a total correction of $(+4 \pm 1.5)\%$ or 20 ± 8 events.

D. Unclassified Events

1. *Ambiguous Events*

This group finally contained 13 events (see Table I, line 8.1), and in every case the problem was the same. One track of each event had a "heavy" density for a first short length before the track became obviously "electronic," and the classification could equally have been as "heavy" if the characteristics of the track were interpreted as showing a pion or muon decaying to an electron, or as "electronic," when the evidence was interpreted as showing an electron track of high angle of dip

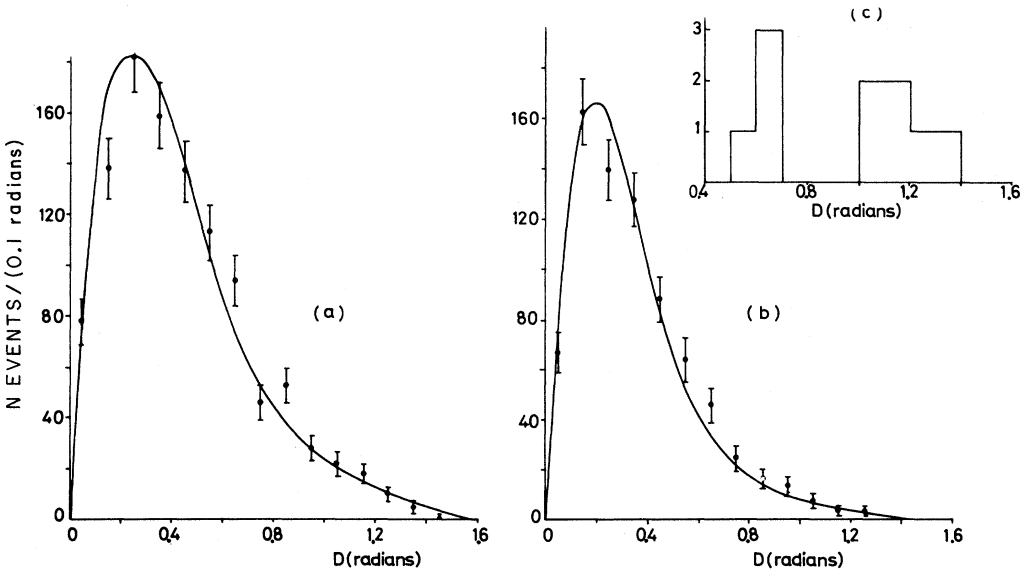

FIG. 5. Distributions in dip for 1836 measured events. The histograms represent the data and the smooth curves the Monte Carlo predictions. (a) shows the distribution for K_{e3} events, (b) for $K_{\mu 3}$, and (c) for the ambiguous events.

scattering into a direction more in the plane of view. Since these events had been considered ambiguous by at least two physicists, the properties of the group as a whole were considered in order to assign them to the K_{e3} and $K_{\mu 3}$ categories. The properties studied for this purpose were as follows.

(i) The dip distribution. Some 60% of all events were measured on image-plane measuring machines with on-line geometrical reconstruction of tracks,[17] and for each measured event the quantity D was defined as the dip of that track with the largest absolute value of the dip. The experimental distributions of D for the $K_{\mu 3}$ and K_{e3} events were then compared with the distributions predicted by the Monte Carlo simulation of the experiment [Figs. 5(a), 5(b)]. In both cases the over-all fit was quite good [χ^2 confidence level (C.L.) about 5% for K_{e3}, and about 30% for $K_{\mu 3}$], but attention was concentrated on the $K_{\mu 3}$ distribution since the distribution in dip for electron tracks was not expected to be particularly reliable (see the Appendix). The $K_{\mu 3}$ distribution had a small excess of events with high values of D (for $D > 0.5$, the data contained 174 events, while the prediction was 142), and assignment of the 10 ambiguous events to that mode would have resulted in a worsening of this effect, since all ambiguous events had $D > 0.5$ [Fig. 5(c)]. This was particularly marked for those events with $D > 1.0$; in this region the $K_{\mu 3}$ data contained 13 events, in agreement with the Monte Carlo prediction of 13, while there were 6 such ambiguous events. In conclusion, therefore, the assignment of all 10 ambiguous events in this measured sample to the $K_{\mu 3}$ mode would have worsened the fit for $D > 0.5$ from a χ^2 C.L. of 1% to one of 0.05%, or for $D > 1.0$ from a χ^2 C.L. of 100% to one of about 8%, and this was taken as indicating that the ambiguous events should be properly classified with the K_{e3} mode.

(ii) The track length. The initial short portion of each of the 13 ambiguous tracks, which might have been muon or pion tracks leading to a decay, had a projected length less than 5 cm. The number of $K_{\mu 3}$ decays with a projected track length this short predicted by the Monte Carlo simulation was somewhat sensitive to the low-energy part of the K_L^0 beam momentum spectrum, and was estimated to lie in the range 80–100. Since the $K_{\mu 3}$ data contained 79 such short decaying tracks, this test allowed no conclusion to be drawn concerning the correct assignment of the ambiguous events.

(iii) Comparison with known electrons. The only feature of the tracks which caused them to be classified as ambiguous was the apparent heavy ionization over the first short part of the track. However, a study of γ-ray pairs in the liquid revealed many examples of steeply dipping tracks with just such characteristics as distinguished those under discussion. It is well known that ionization information may be deceptive for steeply dipping tracks, and normally a cut on dip would be applied. This was not used in this case, since for the vast majority of tracks the ionization information was not important for the identification.

In that the statistical tests on the nature of the ambiguous events were not conclusive, for their final assignment they were allocated to the decay modes in proportion to the $K_{\mu 3}/K_{e3}$ branching ratio. Thus, eight events were added to the K_{e3} category, and five to the $K_{\mu 3}$. In fact, if they were all to be added to one decay mode, or to the other, the effect on the branching ratio finally derived would be less than $\frac{1}{3}$ of the final error.

2. *Unassigned Events*

In this class of event, one of the tracks in a decay reentered the pipe before identification was possible. Of the four events (Table I, lines 8.2–8.4), one with an associated γ was assigned to $K_{3\pi}$, one with an identified electron was assigned to K_{e3}, and the remaining two assigned one each to K_{e3} and $K_{\mu 3}$.

E. Single-Track Events Without Associated γ Rays; Effects of Pion and Muon Decay in the Pipe Wall

Single-track events without associated γ rays arose in two independent ways.

1. *Geometrical Loss*

Here the unseen track emerged from the pipe so far from the seen track that it was outside the visible region. Those single tracks which arose from loss of the upstream track came from events which, had both tracks been seen, would by definition have been outside the fiducial region. Those events where the single seen track *was* the upstream track, and the downstream track had emerged outside the visible region, were within the defined fiducial region, but this correction is part of that derived under the "geometrical detection efficiency" (Sec. IV B).

2. *Pipe-Wall Effects*

Here the unseen particle was absorbed in some way, or stopped in the aluminum wall of the pipe. There were three processes which could have given rise to this absorption:

(i) Stopping of those pions and muons which did not have enough energy to pass through the pipe wall. The magnitude of the correction necessary to take account of this process was obtained from the Monte Carlo calculation. For this it was as-

TABLE IV. Single-track assignments, and effects of pion and muon decay in the pipe wall.

	Track-loss mechanism	Resultant single-track events: Pions identified	Pions unidentified	Muons	Electrons	$K_{\mu 3}$ as K_{e3}	K_{e3} as e^+e^-	Total
	Geometrical loss (calculated from the Monte Carlo simulation) of one track in:							
1	K_{e3}	29.0±2.5	17.0±1.8	···	12.0±1.2	···	···	58.0±3.3
2	$K_{\mu 3}$	7.0±0.5	4.0±0.3	6.0±0.5	···	···	···	17.0±0.8
	Stopping of pions in the pipe wall (calculated from the Monte Carlo simulation):							
3	K_{e3}	···	···	···	12.0±2.0	···	12.0±2.0	24.0±3.0
4	$K_{\mu 3}$	···	···	6.5±1.0	···	6.5±1.0	···	13.0±2.0
5	Stopping of muons in the pipe wall (calculated from the Monte Carlo simulation)	4.5±0.5	2.5±0.2	···	···	14.0±2.0	···	21.0±2.5
	Interaction of pions in the pipe wall, with no visible secondary (estimated from the data):							
6	K_{e3}	···	···	···	6.0±2.0	···	···	6.0±2.0
7	$K_{\mu 3}$	···	···	3.0±1.0	···	···	···	3.0±1.0
8	Total of lines 1–7	40.5±3.0	23.5±2.0	15.5±1.5	30.0±3.0	20.5±2.0	12.0±2.0	142.0±6.0
9	Data (after correction for scan efficiency = 0.9)	52.0±8.5	39.0±7.0		45.5±8.0	···	45.0±7.0	180.5±16.0
10	Absorption of electrons in the pipe wall [see Sec. IV E 2 (iii)]	11.5±9.0	7.0±5.0		···	···	···	18.5±10.0

sumed that all positive pions and muons, and 33% [18] of the negative muons, which had insufficient energy to pass through the pipe wall, decayed producing an electron, which would have been seen and recorded as such. Because of this, some $K_{\mu 3}$ events would have appeared as K_{e3}, and some K_{e3} events as e^+e^- events. All negative pions and the remaining negative muons would have been absorbed, giving no visible decay electron, and so resulting in single-track events. The results of these calculations are given in Table IV, lines 3–5. In the data there was an excess of e^+e^- events over those expected from this source, which was attributable to γ-ray conversion in the pipe wall or in the residual gas in the pipe.

(ii) Interaction of pions in the pipe wall. This could have led either to the rejection of an event at the scanning stage, or to a single-track event, depending on whether or not charged secondaries from the interaction entered the liquid. To estimate the effect of these interactions, the number and type of any pion interactions in the first 5 cm (projected) of path after emerging from the pipe were tabulated for all events. It was found that 63 of the pions from 1890 K_{e3} events interacted in this region to give more than one charged secondary, compared with a total of 36 from 1309 $K_{\mu 3}$ events and 34 from 558 $K_{3\pi}$ events; about 10% of such interactions, had they occurred in the wall of the pipe, would not have given rise to visible secondaries. Assuming that pion interactions in aluminum have similar characteristics to those in Freon, adjusting the interaction probability according to the ratio of the natural collision lengths in Freon and aluminum, and taking (from the Monte Carlo simulation) the mean path length for pions in the pipe wall to be 0.89 cm for K_{e3}, 0.92 cm for $K_{\mu 3}$, and 0.94 cm for $K_{3\pi}$, there would have been a loss of 20 K_{e3} events, 12 $K_{\mu 3}$ events, and 12 $K_{3\pi}$ events due to the application of the "not more than two tracks" criterion in the scan rules. Further, those interactions giving no visible secondaries would have led to single-track events. The number of such events in the experiment was estimated from the study of pion interactions in the liquid to be about six single electrons from K_{e3} decays and three single muons from $K_{\mu 3}$ decays.

(iii) Electron absorption processes. It was more difficult to calculate the magnitude of this effect directly, and so the following approach was adopted. The number of single pions, N_π^s, which should have arisen from the processes described above [Secs. IV E 1 and IV E 2 (i)] was calculated to be 64, and using the experimentally determined pion identification efficiency $P_\pi = 0.63$, the number of these which should have been identified as pions was $N_{\pi,i}^s = P_\pi N_\pi^s = 40.5$ events (sum of lines 1, 2, and 5, column 1, Table IV). This number was subtracted from the total number of identified pions in the data ($N_{\pi,i}^{\rm obs} = 47$ events), taking into account the scanning efficiency for single-track events ($\epsilon_s = 0.9$), and the remainder, $N_{\pi,i}^e = N_{\pi,i}^{\rm obs}/\epsilon_s - N_{\pi,i}^s = 11.5$ (line 10, column 1, Table IV), were then taken as those single identified pions arising from the loss of the electron in the pipe wall. The total correction to be applied from this process was then just $N_{\pi,i}^e/P_\pi = 18.5$ events. The number of single-track events expected from each source is compared with the number actually observed in Table IV.

F. Single-Track Events with Associated γ Rays

Such events arose primarily from two sources: (i) $K_{3\pi}$ decays in which one of the charged pions was lost geometrically or by absorption as outlined in the previous section, and (ii) K_{e3} events in which the electron was annihilated or totally radiated in the pipe wall, the conversion pairs being detected. It was calculated that 11 of the 19 events in which a single nonelectronic track and two conversion pairs were observed, and three of the 16 events with a single conversion pair, arose from process (i). Allowing for not more than two events from $K_{\mu 3}$ in which the pion interacts in the pipe wall to give a π^0, the remaining 6 ± 5 events with two γ rays and 13 ± 4 events with a single γ ray were attributed to process (ii).

G. Unassociated Tracks

Since the decay vertex was not seen in this experiment, the assumption was made that, if two tracks of oppositely charged particles were seen to emerge from the pipe within the fiducial region, then those two particles came from a single decay of the K_L^0. The possibility that two charged tracks of opposite sign and satisfying the criteria could have arisen from two decays had to be considered. The effect was estimated from the data as follows.

The number of "events" where two tracks of the *same* charge were observed to satisfy the criteria obviously came from two decays. The possibility of occurrence of two such tracks of opposite sign must be the same as that of two tracks of the same sign. In the data, there were four events recorded with both tracks having the same charge (three π^+e^+ and one t^-t^-), and hence four events would have been expected where tracks of the opposite sign arose from different decays; three of these should have been $\pi^\pm e^\mp$ and one t^+t^-. In fact, three such "πe" events and one such "t^+t^-" event were recorded by the physicist as seemingly unassociated. From this study, then, no further unassociated events would be expected in the remaining data.

H. Unassociated γ Rays

γ rays could arise from several sources unconnected with an otherwise valid decay in the chamber, and if spatially consistent with the likely vertex of the charged tracks would have changed the visible topological character of an event and so its classification. Thus, a $K_{\mu 3}$ decay with an extraneous γ ray would have been classified as a $K_{3\pi}$ decay, and a K_{e3} decay under the same conditions would have been placed in the category tentatively assigned to radiative K_{e3} decays. In order to evaluate the magnitude of this effect the scan rules were designed to collect events of the type "two heavy tracks and three possibly associated γ rays" ($K_{3\pi}$, 3γ). Such events would have arisen from the coincidence of a $K_{3\pi}$ decay with two associated γ rays ($K_{3\pi}$, 2γ) with a third, unassociated γ ray. There was a single event of the $K_{3\pi}$, 3γ type found, in a total of 446 $K_{3\pi}$, 2γ events, from which a probability of $(0.2 \pm 0.2)\%$ of incorrectly associating a γ ray with an event was found. However, there was a possibility that this calculation would only give a lower limit on the effect on the data of unassociated γ rays, since the probable decay vertex was much more closely defined for a $K_{3\pi}$, 2γ event than for a $K_{\mu 3}$ event, and so it would have been more likely for an unassociated γ ray to be accepted as "possibly associated" in the latter case than in the former. For this reason, a subsidiary scan of about 1200 frames was carried out, recording all frames with either no event of any nature within the fiducial region or with only a single γ ray which, had there been an event anywhere in the fiducial region, would have been consistent with the vertex of such an event. In 400 "no-event" frames, nine γ rays were found; that is, the probability that a γ ray unconnected with any accepted event appeared to come from the pipe was about one in 45 frames, and since the vertex of an event

TABLE V. Corrections and assignment of events to the K_{e3}, $K_{\mu 3}$, and $K_{3\pi}$ classes.

Section	Description	K_{e3}	$K_{\mu 3}$ $\pi^+\pi^-$	$K_{3\pi}$
	Identified events	1890	1309 8	558
IV A	Scanning and identification efficiency [a]	+70 ± 41	0	+50 ± 23
IV B	Geometrical detection efficiency	0 ± 19	0 ± 13	−21 ± 6
IV C 1	γ-detection efficiency	...	−8 ± 2	+8 ± 2
IV C 1	$\pi^+\pi^-$ decay mode	...	−8	...
IV C 2	Dalitz pairs	...	...	+7
IV C 3	Electrons on pipe	...	...	+22 ± 8
IV D 1	Ambiguous	+8 ± 5	+5 ± 5	0
IV D 2	Unidentified	+2	+1	+1
IV E 2 (i)	Pion and muon decay in pipe wall	+24 ± 3 −20.5 ± 2	+34 ± 3.5	+10 ± 1
IV E 2 (ii)	Pion interactions in pipe wall	+26 ± 3	+15 ± 2	+15 ± 2
IV E 2 (iii)	Electron absorption processes with no converted bremsstrahlung	+18.5 ± 10	...	...
IV F	Electron absorption processes with converted bremsstrahlung	+19 ± 6	...	...
IV H	Unassociated γ rays	...	...	−5 ± 2
IV I	Radiative decays	+11 ± 4	...	...
	Totals after corrections	2047.5 ± 63	1348 ± 39	645 ± 35

[a] Normalized to 100% for $K_{\mu 3}$ decays.

could be located on the scan table to about ±6 cm, the probability of a false association of a γ ray with the vertex of an event was about 0.4%.

The possible sources of such γ rays from other K_L^0 decays both in and upstream of the fiducial region were considered, and the total probability evaluated was quite consistent with these figures. Thus five events were calculated to arise from the incorrect association of a $K_{\mu 3}$ event with a γ ray, and were subtracted from the $K_{3\pi}$ sample. Because such events have evidence for two decays on the same frame they do not fall within the accepted sample and so were not added to the $K_{\mu 3}$ mode. There were calculated to be 8 K_{e3} events with an additional γ ray arising from this source; these are considered in the next section.

I. Radiative K Leptonic Decays

In the scanning, 19 events were found where an electron and a heavy track (presumed to be a pion) appeared to be associated with a γ ray from a possible origin for the event. After subtraction of the expected background in the manner outlined in Sec. IV H, 11 events remained, and these were assigned to the radiative decay $K_L^0 \to \pi e \nu \gamma$ ($K_{e3,\gamma}$).[19] Since there was a clear separation of the radiative and nonradiative K_{e3} decays only for those configurations where the radiative γ rays could not be confused with bremsstrahlung from the electron, the sample of K_{e3} decays already contained many radiative decays. Also, most other experiments have not materialized the photons, and so the distinction between radiative and nonradiative decays is lost. For these reasons, the radiative events were added into the K_{e3} sample. No correction has been made for the $K_{\mu 3,\gamma}$ events since the expected rate is extremely low.

J. Sensitivity of the Corrections to the Values of ξ and a_0

Some of the corrections evaluated in the previous sections were obtained by making use of a Monte Carlo simulation of the experiment. In this simulation the value of $\xi = 0.0$ was used to generate the K_{l3} decays. The possibility that a different value of ξ would have led to appreciably different corrections was investigated. For this purpose, the Monte Carlo simulation was repeated with values of $\xi = -1.0$, and $+1.0$, and the corrections reevaluated. Assuming that the *difference* in the magnitudes of the corrections is a linear function of $|\xi|$ over this region, the following were obtained:

(i) The geometrical detection efficiency for $K_{\mu 3}$ events changes with ξ according to

$$\Delta \epsilon_{K_{\mu 3}}^{\text{geom}} / \Delta |\xi| = \Delta (N_{K_{\mu 3}}^{\text{obs}} / N_{K_{\mu 3}}^{\text{true}}) / \Delta |\xi| = \alpha,$$

where $\alpha = -0.03 \pm 0.02$.

(ii) The number of stopping pion and muon tracks in the pipe wall [Sec. IV E 2 (i)] changes with ξ according to $\Delta (N_{\text{stop}}) / \Delta |\xi| = \beta$, where $\beta = 0.0 \pm 0.004$. With the $K_{\mu 3}/K_{e3}$ branching ratio (R_1) found in this experiment, the value deduced for ξ was ~ -0.4. The total correction to R_1 arising from the ξ-dependent effects was then $(1.2 \pm 0.8)\%$. This is four times smaller than the purely statistical error, and has not been included since other unknown systematic effects in the calculation were almost certainly of comparable magnitude.

The sensitivity of the branching ratio $R_2 = (K_L^0 \to \pi^+ \pi^- \pi^0)/(K_L^0 \to \text{all charged})$ to a_0 was similarly investigated, with the result $dR_2/da_0 = 0.0 \pm 0.014$.

K. Conclusion of Sec. IV.

The results of the corrections of this section are given in Table V. The final corrected branching ratios are then

$$R_1 = \frac{K_L^0 \to \pi \mu \nu}{K_L^0 \to \pi e \nu} = 0.662 \pm 0.030,$$

$$R_2 = \frac{K_L^0 \to \pi^+ \pi^- \pi^0}{K_L^0 \to \text{all charged modes}} = 0.159 \pm 0.010,$$

where the errors have been obtained by the quadrature sum of the statistical error (about ±0.025 for R_1) and the estimated errors in the corrections. There has been no further factor folded in to account for possible unknown systematic biases.

V. DISCUSSION

In Table VI the results of recent measurements of R_1 and R_2 are summarized. The value of R_2 obtained in this experiment is in good agreement with other measurements, while the value of R_1 is somewhat lower than in most previous work. With the exception of other heavy-liquid bubble-chamber measurements,[20,21] previous experiments have had to deal with the difficulty of a variable detection efficiency over the Dalitz plot, or have had to fit certain observed distributions, such as total transverse momentum, to a Monte Carlo calculation, using the value of R_1 as a parameter, or have used a combination of these two methods. Such determinations may be sensitive to the form of the interaction, and to the assumptions regarding subsidiary variables, such as the beam momentum spectrum (few experiments have been performed with even approximately monoenergetic K_L^0 beams). In this experiment there are no explicit cuts on the Dalitz plot, nor are there any large cuts on the laboratory momenta of the par-

TABLE VI. Measurements of (a) $(K_L^0 \to \pi\mu\nu)/(K_L^0 \to \pi e\nu)$ and (b) $(K_L^0 \to \pi^+\pi^-\pi^0)/(K_L^0 \to \text{all charged modes})$.

(a)

$R_1(K_{\mu 3}/K_{e3})$	ΔR_1	Method	Reference
0.81	0.19	Hydrogen bubble chamber (HBC)	a
0.73	0.15	HBC	b
0.82	0.10	Spark chamber (SC)	c
0.70	0.20	HBC	d
0.81	0.08	HBC	e
0.71	0.05	Heavy-liquid bubble chamber (HLBC)	f
0.70	0.04	HLBC	g
0.62	0.05	SC	h
0.662	0.030	HLBC	This work

(b)

$R_2\left(\frac{K_L^0 \to \pi^+\pi^-\pi^0}{K_L^0 \to \text{all charged}}\right)$	ΔR_2	Method	Reference
0.151	0.020	HBC	a
0.157	0.030	HBC	b
0.150	0.030	Cloud chamber (CC)	i
0.159	0.015	CC	j
0.178	0.017	HBC	k
0.162	0.015	HBC	d
0.161	0.005	HBC	e
0.159	0.010	HLBC	This work

[a] R. K. Adair and L. B. Leipuner, Phys. Letters 12, 67 (1964).
[b] D. Luers *et al.*, Phys. Rev. 133, 1276 (1964).
[c] X. de Bouard *et al.*, Nuovo Cimento 52A, 662 (1967).
[d] C. J. B. Hawkins, Phys. Rev. 156, 1444 (1967).
[e] H. W. K. Hopkins *et al.*, Phys. Rev. Letters 19, 185 (1967).
[f] I. A. Budagov *et al.*, Nuovo Cimento 57A, 182 (1968).
[g] P. Beillière, G. Boutang, and J. Limon, Phys. Letters 30B, 202 (1969).
[h] P. Basile *et al.*, Phys. Rev. D 2, 78 (1970).
[i] P. Astbury *et al.*, Phys. Letters 16, 80 (1965).
[j] P. Astbury *et al.*, Phys. Letters 18, 175 (1965).
[k] P. Guidoni *et al.*, Argonne Conference Report, 1965.

ticles (the wall of the vacuum pipe absorbs those particles with very low energy, but these form less than 2% of all particles. Furthermore, as discussed in Sec. IV I, the corrections to the measured value of R_1 are not particularly sensitive to the value of ξ [$(dR/d|\xi|)_{\lambda_\pm=0}$ is of the order -0.03 ± 0.02, for $|\xi| \leq 1.0$, unless the form of the interaction is very different from pure $V-A$].

Assuming pure $V-A$ coupling and electron-muon universality, the branching ratio R_1 is given by[22]

$$R_1 = \frac{0.6452 + 3.5467\lambda_+ + 0.1245\,\mathrm{Re}\,\xi(0) + 0.4371\xi(0)(\lambda_+ + \lambda_-) + 0.0187|\xi(0)|^2 + 0.1525|\xi(0)|^2\lambda_- + \cdots}{1 + 3.4571\lambda_+ + \cdots}. \quad (5.1)$$

To extract a value of $\xi(0)$ from this relationship, values for λ_+ and λ_- need to be specified. There have been a number of experiments[1] to measure λ_+ in both K_L^0 and K^+ semileptonic decays, and, although the earlier experiments gave good agreement with the theoretically expected value of $\lambda_+ \sim 0.023$ [calculated assuming dominance of the P-wave amplitude by the $K^*(890)$], recent measurements[23] report a higher value of λ_+, in the region 0.06–0.08, and it is not clear which value of λ_+ is more correct. This is particularly serious since $d\xi(0)/d\lambda_+ \approx -12$ for branching-ratio measurements of $\xi(0)$. We take λ_+ to lie in the range 0.02–0.08.

There have been no measurements of λ_- as yet, but certain theoretical considerations[24] require the product $|\lambda_-\xi(0)|$ to be less than 0.01. Using this value as an upper limit, and assuming the reality of ξ,[25] Eq. (5.1) may be solved for $\xi(0)$. The resulting $R_1 - \xi(0)$ relationship for different values of λ_+ is shown in Fig. 6. With the assumption that $\lambda_- = 0$ we obtain

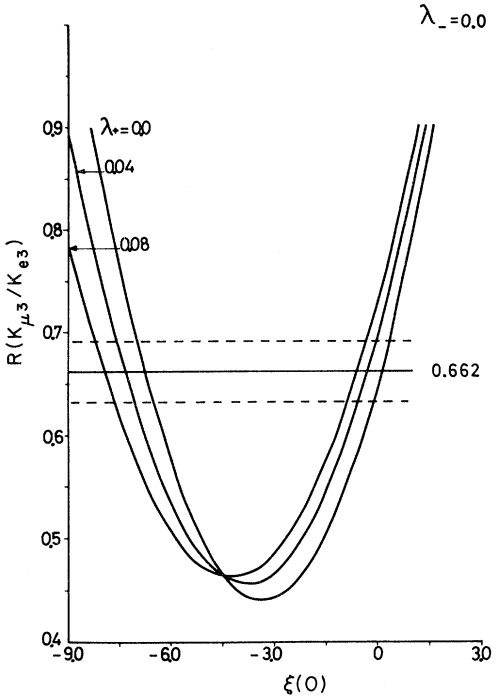

FIG. 6. Variation of branching ratio with $\xi(0)$ for different values of λ_+, evaluated from Eq. (5.1) with $\lambda_- = 0$.

$$\xi(0) = -0.08 \pm 0.25 \quad \text{for } \lambda_+ = 0.02,$$

$$\xi(0) = -0.77 \pm 0.30 \quad \text{for } \lambda_+ = 0.08,$$

the corresponding results for $\lambda_- \xi(0) = +0.01$ and -0.01 being virtually indistinguishable.

Recent measurements of $\xi(0)$ for K^+ and K_L^0 decays, using the Dalitz plot and polarization of the muon in $K_{\mu 3}$ decays together with the conditions under which $\xi(0)$ has been calculated, are shown in Table VII. There is still some discrepancy between the various methods of determining $\xi(0)$. Obvious weaknesses in the derivation of $\xi(0)$ in this case are the uncertainty in λ_+ and the complete lack of knowledge about λ_-. These need to be better known before firmer conclusions can be reached. If indeed the measurements which have indicated a value of $\lambda_+ \sim 0.08$ are correct, then the assumption that $\lambda_+ t/m_{\pi^+}{}^2$ is small, made in deriving Eq. (5.1), no longer holds (the maximum value of this is ~0.5 for $\lambda_+ \sim 0.08$). Furthermore, there is the possibility that the linear expansion of $f_+(t)$ may not be valid, and that second- or higher-order terms might be necessary. However, there have been a number of interesting suggestions to explain the discrepancy. For example, Rajasekaran and Sarma[26] discuss the possibility of a breakdown in the validity of electron-muon universality in strangeness-changing decays, and several authors point out that relatively large departures from pure $V-A$ coupling of the weak currents[27] are not excluded by presently available experimental data. It is not, of course, possible yet to say categorically that there is a discrepancy while reliable values are not available for λ_+ and λ_-.

ACKNOWLEDGMENTS

We are grateful to Professor N. Feather, Professor C. A. Ramm, and Professor A. Rousset for providing the facilities of their departments and for their encouragement and support of this work.

We also wish to thank the staff of the CERN proton synchrotron, the 1.1 m^3 heavy-liquid bubble chamber, and the scanning and measuring staffs at CERN and Edinburgh University, without whose endeavors this experiment would not have been possible.

APPENDIX: THE MONTE CARLO CALCULATION

The essential features of the Monte Carlo simulation of the experiment are described in this appendix. The simulation was programmed in CERN FORTRAN for the CDC 6600 computer at CERN.

The event-generation procedure started with the choice of a beam momentum from the input momentum spectrum determined from $K_{3\pi}$ decays.[5] A point in phase space was then defined by two random numbers representing the energies of the two charged particles in the decay; energy-momentum conservation was imposed, and the form of the decay interaction taken into account by determining the value of the squared matrix element at the point chosen, comparing it with the maximum possible value, and accepting or rejecting the events according to another random number. For K_{e3} decays Eq. (1.2) with constant form factors was used, while for $K_{3\pi}$ decays the form

$$|M|^2 \sim 1 + 2a_0(m_K/m_{\pi^+}{}^2)T_{\max}(2T_0/T_{\max} - 1)$$

was employed. For an accepted event, the direction of the charged lepton (or π^+ in $K_{3\pi}$ decays) was distributed uniformly over the surface of a sphere, and the charged-pion direction was distributed isotropically in rotational angle about the charged-lepton direction. The other angles in the decay were determined by kinematical relations.

A Lorentz transformation of the particle momenta to the laboratory system was carried out using the known kaon momentum, and the decay vertex was chosen to lie uniformly in a circle of 2-cm diameter about the beam axis in the yz plane, and uniformly in the x direction from $x = -35$ to $x = +65$ cm. There was no allowance for beam attenuation by decay, since such attenuation would

TABLE VII. Determination of $\xi(0)$ from K^+ and K^0 experiments.

$\xi(0)$	K^+/K^0	Method	Conditions, assumptions, comments	Technique	Reference
$-0.54^{+0.4}_{-0.5}$	K^0	Branching ratio	$\lambda_+=0.023$, $\lambda_-=0.0$	SC	a
$+0.3\pm0.4$	K^0	Branching ratio	$\lambda_+=0.023$, $\lambda_-=0.0$	HLBC	b
$+0.8\pm0.5$	K^+	Branching ratio	$\lambda_+\sim\lambda_-\sim 0.0$	HLBC/HBC	c
$+0.4\pm0.4$	K^+	Branching ratio	$\lambda_+=\lambda_-=0.0$	HLBC	c
$+0.75\pm0.5$	K^+	Branching ratio	$\lambda_+=\lambda_-=0.0$	SC	e
-0.72 ± 0.2	K^+	Branching ratio	$\lambda_+=0.029$ measured at $t=4\,m^2$	HLBC	f
-0.35 ± 0.22	K^+	Branching ratio	$\lambda_+=0.045$, $\lambda_-=0.0$	SC	g
-3.9 ± 0.1 / $+1.5\pm0.2$	K^0	Dalitz plot	ξ assumed constant; of the two values $\xi=-3.9$ is favored.	SC	a
$-0.68^{+0.12}_{-0.20}$	K^0	Dalitz plot	$\lambda_+=0.09$, $\lambda_-=0.0$	SC	h
-2.5 ± 0.65	K^0	Dalitz plot	$\lambda_+=0.078\pm0.013$, $\lambda_-\sim 0.07$, $d\xi/d\lambda_+\sim-50$	SC	i
-1.1 ± 0.5	K^+	Dalitz plot	$\lambda_+=0.050\pm0.019$, $\lambda_-=0.0$	HLBC	j
-1.2 ± 0.5	K^0	Polarization	$\lambda_+=0.0$	SC	k
-1.6 ± 0.5	K^0	Polarization	$\lambda_+=\lambda_-=0.0$	SC	l
$-1.81^{+0.5}_{-0.2}$	K^0	Polarization	$\lvert\lambda_+\rvert<0.1$, quoted for $\lambda_+=\lambda_-=0.0$	SC	m
-1.0 ± 0.3	K^+	Polarization	Measured at $t=4.9\,m_\pi^2$	HLBC	j
-0.95 ± 0.3	K^+	Polarization	$\lambda_+=\lambda_-=0.0$	SC	h
-0.08 ± 0.25 / -0.77 ± 0.30	K^0	Branching ratio	$\lambda_+=0.02$ / $\lambda_+=0.08$, $\lambda_-=0.0$; insensitive to λ_-	HLBC	This exp.

[a] See Table VI, Ref. h.
[b] See Table VI, Ref. f.
[c] V. Bisi *et al.*, Phys. Rev. 139, B1068 (1965).
[d] A. C. Callahan *et al.*, Phys. Rev. 150, 1153 (1966).
[e] L. B. Auerbach *et al.*, Phys. Rev. 155, 1505 (1967).
[f] T. Eichten *et al.*, X2 Collaboration, Phys. Letters 27B, 586 (1968).
[g] D. R. Botterill *et al.*, Phys. Letters 31B, 325 (1970).
[h] C. Y. Chien *et al.*, Phys. Letters 33B, 627 (1970).
[i] D. Aston *et al.*, Daresbury Report No. DNPL/R 9, 1971 (unpublished).
[j] D. Haidt *et al.*, X2 Collaboration, Phys. Rev. D 3, 10 (1971).
[k] L. B. Auerbach *et al.*, Phys. Rev. Letters 17, 980 (1966).
[l] R. J. Abrams *et al.*, Phys. Rev. 176, 1603 (1967).
[m] M. J. Longo *et al.*, Phys. Rev. 181, 1808 (1969).
[n] D. Cutts *et al.*, Phys. Rev. Letters 20, 955 (1968).

be less than 2% over the fiducial region and would not be observable with the limited statistics available. The points of intersection of the charged track orbits with the inside and outside of the pipe wall were found by an iterative procedure, stepping down the circular helical tracks until they reached the appropriate radius. The magnetic field in the pipe was assumed constant over the whole decay region; this was not correct for the decay vertices in the region $x<-25$ cm,[28] but the effect on the predictions of changing the magnetic field is very small. The track length in the wall of the pipe was compared with the total range for that momentum, and the track was identified as stopping in the pipe wall if the thickness of aluminum to be traversed was greater than the range. In this simulation no account was taken of nuclear interactions in the pipe wall, but the effects of multiple scattering were included by changing the direction of the track according to the approximate multiple-scattering formula

$$\langle\theta\rangle=\{2.12/P_i\beta_i\}^2\times d_{\rm Al}/X_{\rm Al}\,.$$

Pion and muon tracks were followed stepwise through the liquid to determine whether they stopped, or interacted, or left the chamber. Interactions were simulated for pions by using a momentum-dependent interaction length for $\pi^\pm$ in Freon of the form

$$l_\pm(p)=28a_\pm[10^{\alpha(p-p_{\rm min})}+10^{\beta(p-p_{\rm min})}]\,,$$

with $a_+=0.84$, $a_-=1.0$, $\alpha=-5.0$, $\beta=+3.0$, and $p_{\rm min}=0.275$ GeV/c.[29] Particles with momentum greater than 0.5 GeV/c were given a constant collision length, with p in the above formula set to 0.5 GeV/c. The constants $a_\pm$, α, and β were adjusted to give quantitative agreement for the number of pion interactions in $K_{3\pi}$ decays. γ rays from π^0 in $K_{3\pi}$ decays were generated isotropically in the

π^0 rest system, Lorentz transformed to the laboratory system, and "converted" in the chamber, with a conversion length of 14.1 cm. Low-energy (<20 MeV) γ rays were given a conversion length equal to $14.1\times(20/E_\gamma)$. Conversion in the pipe wall was approximated by the same method, with a conversion length of 11.0 cm.

The track variables were perturbed according to a Gaussian distribution with half-width given by the expected errors arising from multiple scattering and measurement setting.[30] For nonstopping tracks of length <15 cm, the calculated track length was used, but for those with track length >15 cm, the length was assumed to be uniformly distributed between 15 and 30 cm; the results were not sensitive to the exact nature of these assumptions. For electrons it was assumed that for those with a radius of curvature <15 cm a track length equal to the radius of curvature would have been measured. No account was taken of bremsstrahlung emission, which in principle alters only the energy, so that the dip angle of the electron is maintained.

Generated events could be output either in scan-card format for analysis by the scan-card analysis program, or in geometry records in identical format to the measurements.

---

*Work supported in part by the Science Research Council of Great Britain.

†Visitor from Laboratory for Nuclear Problems, Joint Institute for Nuclear Research, Dubna, USSR.

‡Visitor from University of Aachen, Aachen, Germany.

§Now at National Accelerator Laboratory, Batavia, Ill., U.S.A.

‖Visitor from University College, London, England.

[1]A recent compilation containing many references to experimental and theoretical work on this subject has been made by M. K. Gaillard and L. M. Chounet [CERN Report No. 70-14, 1970 (unpublished)].

[2]See, for example, J. D. Jackson, *Elementary Particle Physics and Field Theory 1* (Benjamin, New York, 1963).

[3]G. R. Evans, M. Golden, J. Muir, K. J. Peach, I. A. Budagov, H. W. K. Hopkins, W. Krenz, F. A. Nezrick, and R. G. Worthington, Phys. Rev. Letters 23, 427 (1969).

[4]I. A. Budagov, D. C. Cundy, G. Myatt, F. A. Nezrick, G. M. Trilling, W. Venus, H. Yoshiki, B. Aubert, P. Heusse, I. Le Dong, J. P. Lowys, D. Morellet, E. Nagy, C. Pascaud, L. Behr, P. Beillière, G. Boutang, and M. Schiff, Phys. Rev. D 2, 815 (1970).

[5]H. W. K. Hopkins, W. Krenz, G. R. Evans, J. Muir, and K. J. Peach, Bull. Am. Phys. Soc. 16, 18 (1971); Lett. Nuovo Cimento 4, 213 (1972).

[6]These numbers were derived from the study by Gerber *et al.*, of neutral particles at 30° from the Brookhaven AGS: H. J. Gerber, G. Fischer, R. Jones and A. Wattenberg, University of Illinois Technical Report No. 39, 1962 (unpublished).

[7]In this paper, "γ ray" will normally refer to the observation of a conversion pair or Compton electrons.

[8]Since this is a purely scanning experiment, the scan-region limitations were initially defined for convenience in terms of image-plane distances on the scan table. However, all distances quoted in this paper are real-space distances. Where unspecified, positions along the pipe are referred to an origin ($x = 0$) at the upstream mark. In this system, the center of the chamber is at $x = +40$ cm.

[9]D. Morellet, Orsay Report No. LAL 1190 (unpublished).

[10]J. Sawicki and H. Yoshiki, Nuovo Cimento 42, 410 (1966).

[11]Those few single protons which arise from pion interactions in the pipe wall would have been classed as stopping heavy tracks, since it was not always possible to distinguish between such tracks and pion or muon tracks of this nature.

[12]This included those events having two tracks of the same sign, and those with unusual topologies such as $\pi e\gamma$, $\pi\pi 3\gamma$, $\pi^+\pi^-$, etc.

[13]To the best of our knowledge, this technique was first suggested by J. Vander Velde [Ecole Polytechnique Report, 1967 (unpublished)].

[14]S. E. Derenzo and R. M. Hildebrand, Nucl. Instrum. Methods 69, 287 (1969).

[15]We use the world average given by the Particle Data Group [Rev. Mod. Phys. 43, S1 (1971)].

[16]N. P. Samios, Phys. Rev. 121, 275 (1961).

[17]K. Soop, CERN Report No. CERN 68-37, 1968 (unpublished).

[18]This value was derived from muon capture rate data given in R. Klein, Phys. Rev. 146, 756 (1966); see also J. C. Sens, CERN Report No. CERN 66-29, 1966 (unpublished), p. 85.

[19]This decay mode has been treated in a separate publication: K. J. Peach, G. R. Evans, J. Muir, I. A. Budagov, H. W. K. Hopkins, W. Krenz, F. A. Nezrick, and R. G. Worthington, Phys. Letters 35B, 351 (1971).

[20]I. A. Budagov, D. C. Cundy, G. Myatt, F. A. Nezrick, G. M. Trilling, W. Venus, H. Yoshiki, B. Aubert, P. Heusse, I. Le Dong, J. P. Lowys, D. Morellet, E. Nagy, C. Pascaud, L. Behr, P. Beillière, G. Boutang, and M. Schiff, Nuovo Cimento 57A, 182 (1968).

[21]P. Beillière, G. Boutang, and J. Limon, Phys. Letters 30B, 202 (1969).

[22]There are a number of differing expressions in the literature giving the relationship between R_1 and $\xi(0)$. We have chosen to use that given by H. W. Fearing, E. Fischbach, and J. Smith, Phys. Rev. Letters 24, 189 (1970).

[23]D. Haidt, H. Schepers, J. Stein, H. J. Steiner, S. Natali, G. Piscitelli, F. Romano, E. Fett, J. Lemonne, R. Møllerud, T. I. Pedersen, S. N. Tovey, V. Brisson, L. Kluberg, P. Petiau, C. D. Esveld, J. J. M. Timmermans, R. T. Van de Wall, B. Aubert, L. M. Chounet, Dong Lê, F. Bobisut, E. Calimani, S. Ciampolillo,

H. Huzita, D. Gamba, A. E. Werbrouck (X2 Collaboration), Phys.Letters 29B, 691 (1969); D. Haidt *et al.*, Phys. Rev. D 3, 10 (1971). The latter reference contains a detailed comparison of other experimental work together with appropriate references.

[24]See, for example, P. B. Jones, Progr. Nucl. Phys. 12, 1 (1970).

[25]See B. G. Kenney, Lett. Nuovo Cimento 1, 746 (1969) for a discussion of the effects of the nonreality of ξ.

[26]G. Rajasekaran and K. V. L. Sarma, Nucl. Phys. B18, 568 (1970).

[27]See, for example, B. G. Kenney, Phys. Rev. Letters 20, 1217 (1968).

[28]R. Grüb and B. Langeseth, CERN NPA Internal Report No. NPA/Int. 69-16, 1969 (unpublished).

[29]This crude parametrization of the effective cross section was derived using data given by L. Behr, thesis, Paris, 1965 (unpublished).

[30]H. Burmeister and U. Gorsch, CERN NPA internal report, 1968 (unpublished).